Molecular Crystals and Liquid Crystals

ISSN: 1542-1406 (Print) 1563-5287 (Online) Journal homepage: http://www.tandfonline.com/loi/gmcl20

Alignment of Hard Spherocylinders by Hard Spheres on Substrates

Tomonori Koda, Makoto Uchida, Akihiro Nishioka, Osamu Haba, Koichiro Yonetake, Musun Kwak, Yuichi Momoi, Nakwon Kim, Sangpyo Hong, Dongwoo Kang & Youngseok Choi

To cite this article: Tomonori Koda, Makoto Uchida, Akihiro Nishioka, Osamu Haba, Koichiro Yonetake, Musun Kwak, Yuichi Momoi, Nakwon Kim, Sangpyo Hong, Dongwoo Kang & Youngseok Choi (2015) Alignment of Hard Spherocylinders by Hard Spheres on Substrates, Molecular Crystals and Liquid Crystals, 612:1, 24-32, DOI: 10.1080/15421406.2015.1030572

To link to this article: http://dx.doi.org/10.1080/15421406.2015.1030572

Mol. Cryst. Liq. Cryst., Vol. 612: pp. 24–32, 2015

ISSN: 1542-1406 print/1563-5287 online
DOI: 10.1080/15421406.2015.1030572

Taylor & Francis
Taylor & Francis Group

Alignment of Hard Spherocylinders by Hard Spheres on Substrates

TOMONORI KODA,[1,*] MAKOTO UCHIDA,[1]
AKIHIRO NISHIOKA,[1] OSAMU HABA,[1]
KOICHIRO YONETAKE,[1] MUSUN KWAK,[2] YUICHI MOMOI,[3]
NAKWON KIM,[2] SANGPYO HONG,[2]
DONGWOO KANG,[2] AND YOUNGSEOK CHOI[2]

[1]Graduate School of Science and Engineering, Yamagata University, Yonezawa, Japan
[2]Process Development Division, LG Display Co., Ltd., Paju, Korea
[3]Japan Lab., LG Display Co., Ltd., Tokyo, Japan

We performed Monte Carlo simulation of the system consisting of hard spheres, hard spherocylinders and a large hard plate. These elements were used to examine how substrates modified by adsorbed particles affect an alignment of liquid crystal molecules. In order to adsorb the hard spheres on the hard plate, dragging potential for spheres were introduced. We prepared a homogeneous and a homeotropic alignment as an initial configuration of the simulations. Numbers and the size of adsorbed spheres were changed. Results showed that molecular alignment after relaxation depended on the initial configuration even for the same system parameters. We expect that the nematic phase of the present systems favor the homogeneous alignment. This is because we observed cases in which the homeotropic alignment was canceled after relaxation and we never observed cases in which the homogeneous alignment was canceled for the nematic phase of the present systems.

Keywords Monte Carlo simulation; nematic phase; alignment; substrate

1. Introduction

Alignment of liquid crystal molecules is affected by substrate conditions. For liquid crystal displays of these days, a memory imposed by rubbing of polyimide substrate determines the alignment when electric field is off. Photoalignment [1, 2], glancing impingement of ion beam [3], and so on are now in development for post-rubbing techniques.

For one candidate of such techniques, we have recently reported that spontaneous homeotropic alignment by small amount of liquid crystal dendrimers in dissolved nematic material is adopted for display with interdigitated in-plane electrodes [4–6]. Similar idea was also proposed for homeotropic alignment induced by added nanoparticles [7–9]. In the

*Address correspondence to Tomonori Koda, Graduate School of Science and Engineering, Yamagata University, 4-3-16 Jonan, Yonezawa, Yamagata 992-8510, Japan. E-mail: koda@yz.yamagata-u.ac.jp

Color versions of one or more of the figures in the article can be found online at www.tandfonline.com/gmcl.

nematic liquid crystal material, dendrimers adsorbed on substrates act as surface agents modifying interaction between substrates and liquid crystal [4].

In the present study, by using molecular simulation for simple molecular models, we examined how molecules adsorbed on substrates affect liquid crystal alignment. The simple molecular models we used were hard spherocylinders for liquid crystal molecules and hard spheres for molecules adsorbed on substrate. Hard spherocylinders have been studied as model systems that express nematic, smectic and crystal phases [10, 11].

Alignments of liquid crystals on substrates are well utilized to liquid crystal displays. However little is known for the alignment in molecular scale. The purpose of the study is to examine how the particles on substrates affect liquid crystal alignment by performing Monte Carlo (MC) simulation of simple model molecules.

2. Simulation

2.1. Models of Molecules and Substrates

We considered systems consisting of hard spherocylinders, hard spheres and a hard plate. The periodic boundary conditions along x-, y- and z- directions were imposed for the system.

The hard plate is a model for substrates. Two surfaces of the plate behave as facing substrates in the periodic boundary. Size of the hard plate is larger enough than the periodic boundary sizes along yz-plane. The plate was always placed at $x = 0$ with its normal pointing x-direction.

The spherocylinder is a cylinder each end of which is capped with a hemisphere [12]. Its shape is characterized by aspect ratio L/D of its diameter D to the length L of the cylinder part. In the present study, we used the spherocylinder of $L/D = 5$ for the liquid crystal molecule. Number N of the spherocylinders in the system was 1950.

As adsorbed molecules that affect liquid crystal alignment on the plate, we added hard spheres in the system of spheroyclinders and the plate. Number N_S and diameter D_S of the hard spheres were changed.

Intersection between molecules and intersection between molecules and the plate was eliminated in the simulation due to hard repulsive interaction potential Φ:

$$\Phi = \begin{cases} +\infty, & \text{if intersection for molecules and the plate exists,} \\ 0, & \text{otherwise.} \end{cases} \tag{1}$$

For adsorption of spheres on the plate substrates, we used a dragging potential U:

$$U = -\sum_{k=1}^{N_S/2} g x_k + \sum_{k=(N_S/2)+1}^{N_S} g x_k, \tag{2}$$

where x_k is the x-component of position of the k-th sphere, and g is strength of dragging potential. The first term of the right hand side of Eq. (2) drags half of spheres to positive direction of the x-coordinate, and the second term to negative direction. In the periodic boundary along x-direction, half and the other half of spheres were attracted, respectively, to one side and the other side of the hard plate. For the present study, dragging strength was

set as

$$\frac{gD}{k_BT} = 5,$$

where k_B is Boltzmann's constant and T temperature.

2.2. *Simulation Procedure*

Isobaric MC simulation was performed for the present study. Unit step of the present MC simulation consisted of trial movements of $N + N_S$ randomly chosen molecules. Trial movement of system size was performed randomly for about three times per unit MC step. Trial movements of molecules obeyed a Boltzmann factor:

$$\exp\left[-\frac{\Phi + U}{k_BT}\right], \tag{3}$$

and trial movements of the system size obeyed a Boltzmann factor:

$$\left(\frac{L_xL_yL_z}{D^3}\right)^{N+N_S} \exp\left[-\frac{\Phi}{k_BT} - \frac{(p^*)L_xL_yL_z}{D^3}\right], \tag{4}$$

where p^* is a normalized external pressure, L_x, L_y, and L_z are system size (periodic boundary size) along x-, y-, and z-direction, respectively. The shape of the system was always a rectangular parallel piped. For an isotropic system size movement, ratios among L_x, L_y, and L_z were fixed, while for an anistropic system size movement, movements of L_x, L_y and L_z were tried independently.

Equilibrated structures depended on initial configuration of molecules. We examined both homeotropic and homogeneous orientations as an initial configuration.

Large initial system size was prepared keeping size ratios $L_x = 2L_z = 2L_y$. To obtain results from homogeneous initial alignment, spherocylinders were parallel aligned in a direction along the plate surface with spheres in a large initial system. The plate was fixed at origin without movement throughout simulations. Simulations started at pressure $p^* = 2.0$ for parallel spherocylinders with isotropic system size movement. At this first stage of the simulation, we did not change the direction of spherocylinders. After equilibration of the first stage, we removed the constraint on directions to rotate spherocylinders with isotropic system size movement. When the system of spheres and rotating spherocylinders was relaxed for the isotropic system size movement, the anisotropic system size movement was allowed to complete equilibration at $p^* = 2.0$. Configuration of equilibrated structure at $p^* = 2.0$ was used as initial configuration to obtain results at $p^* = 1.9$. Structure at lower pressure was thus successively obtained by following a structure at higher pressure.

We also obtained results from an initial homeotropic alignment in the same manner, except for that we started the simulations with spherocylinders aligned parallel to the normal of the substrate plate.

3. Results and Discussion

Figure 1 shows a snapshot of hard spherocylinders and the plate with spheres of diameter $D_S/D = 3$ after relaxation at $p^* = 1.4$ from an initial homeotropic alignment. Number N_S of the spheres was 88. A state obtained after relaxation at $p^* = 1.4$ was a seed for the simulation at $p^* = 1.3$.

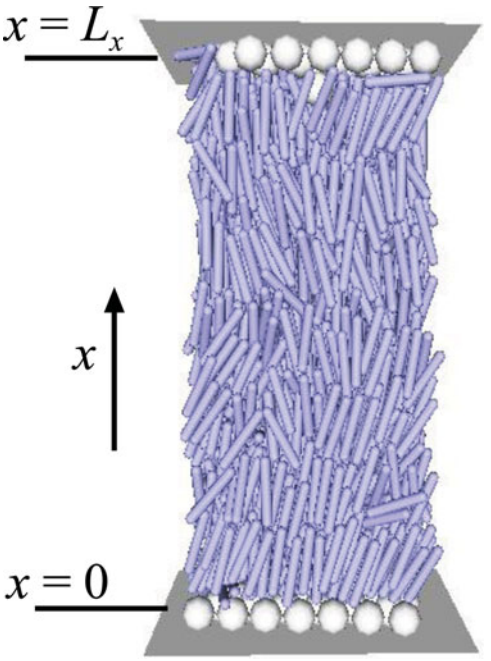

Figure 1. A snap shot of the simulation box of the initially homeotropic structure for $N_S = 88$ and $D_S = 3D$ at $p^* = 1.4$. The plate placed at $x = 0$ also appears at $x = L_x$ according to the periodic boundary condition.

Figure 2 shows a snapshot after relaxation at $p^* = 1.3$. A homeotropic structure of Fig. 1 changed to a structure of Fig. 2. To see the detail of the change from a structure of Fig. 1 to a structure of Fig. 2, we analyzed a structure of the bulk region. We defined that a point was in the bulk region if its distance from the substrates was larger than $10D$. With this definition of the bulk, we calculated the order parameter tensor

$$\mathbf{Q} = \frac{3}{2} < \mathbf{aa} > -\frac{1}{2}\mathbf{u}, \tag{5}$$

of the bulk region, where **a** is a direction of a spherocylinder, **u** is the unit tensor, and a bracket $< >$ is an average for the spherocylinders in the bulk region. We obtained the eigenvector **n** of the largest eigen value of Q as the director in the bulk region. Figure 3(a) shows a change in x-component n_x of the director **n** for $N_S = 88$ and $D_S = 3D$ at $p^* = 1.3$ from initially homeotropic structure. Projection of the director to the normal of the substrate is n_x. Homeotropic alignment corresponds to $n_x = 1$, and homogeneous alignment corresponds to $n_x = 0$. A change from a homeotropic alignment to a tilted alignment is indicated by Fig. 3(a). Figure 3 also shows changes in the alignment from an initially homogeneous structure (Fig. 3(b)) of $N_S = 88$ and $D_S = 3D$. Results from initially homeotropic and homogeneous structures of $N_S = 12$ and $D_S = 8D$ at $p^* = 1.3$ are also shown.

Figure 3 shows cases for simulation parameters $(D_S, N_S) = (3D, 88)$ and $(8D, 12)$. To achieve densely packed structure of hard spheres on substrates, we chose N_S for given D_S

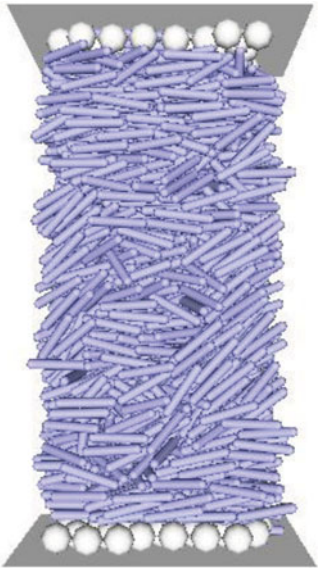

Figure 2. A snap shot of the simulation box of the initially homeotropic structure for $N_S = 88$ and $D_S = 3D$ after relaxation at $p^* = 1.3$.

as the total area

$$A = \pi D_S^2 N_S/4, \tag{6}$$

of spheres projected on substrates satisfied

$$A \cong 628. \tag{7}$$

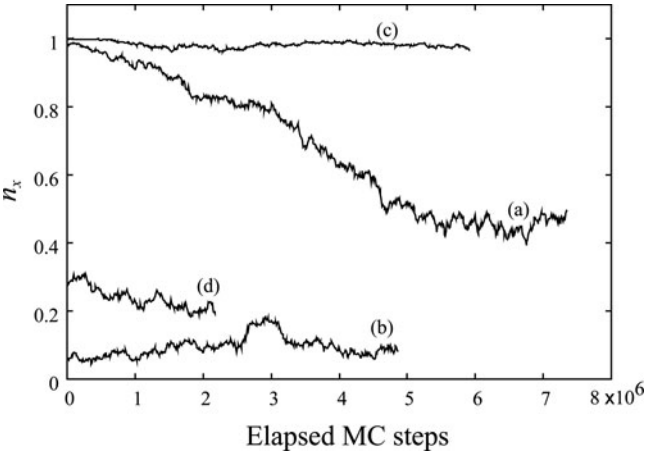

Figure 3. Profiles of x-component of the director in the bulk region at $p^* = 1.3$ from (a) an initially homeotropic strucure of (D_S, N_S) = (3D, 88), (b) an initially homogeneous structure of (3D, 88), (c) an initially homeotropic structure and (d) an initially homogeneous structure of (8D, 12).

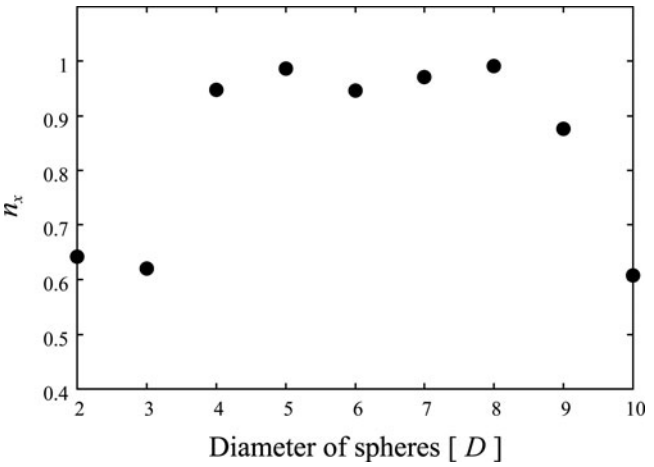

Figure 4. Projection of the bulk director to the normal of substrates when 4×10^6 MC steps was elapsed at $p^* = 1.3$ depending on diameter of spheres. Number of spheres was determined by Eqs. (6) and (7) for the given diameter.

The projections of FIG. 3(c) and (d) of the same system parameters $N_S = 12$ and $D_S = 8D$ went to different values from different initial conditions. A structure after relaxation depended on its initial configuration.

To examine structure from an initially homeotropic alignment, we performed simulations for sets of system parameters $(D_S, N_S) = (2D, 200)$, (3D, 88), $(4D, 50)$, $(5D, 32)$, $(6D, 22)$, $(7D, 16)$, $(8D, 12)$, $(9D, 10)$ and $(10D, 8)$ according to Eqs. (6) and (7). Figure 4 shows n_x at elapsed MC steps 4×10^6 for these sets of system parameters at $p^* = 1.3$. Results of Fig. 4 indicate that stability of the homeotropic alignment $n_x = 1$ increases in the region of sphere diameter between $4D$ and $8D$.

Let us try to explain these results by an excluded volume effect. Figure 5 describes the relation among a sphere, a spherocylinder, the substrate, and the volume excluded by the sphere for the center of the spherocylinder. Distance of the center of a spherocylinder from the substrate is denoted by x. Projection a_x to x-axis of the direction **a** of the spherocyinder is equal to n_x for the case of perfectly aligned spherocylinders. Region bounded by thin solid line around the sphere of Fig. 5 indicates the excluded volume for the spherocylinder by the sphere. The excluded volume region has a shape of spherocylinder of diameter $D_s + D$ and length L. Area σ of intersection of the excluded volume region and a plane of distance x from the substrate is a function of x and n_x.

Due to overlap with the substrate, homeotropic alignment $n_x = 1$ is not allowed for $x < (L + D)/2$, and $n_x = 0$ is not allowed for $x < D/2$. Examining the shape of the spherocylinder we have,

$$\sigma(x, 1) = 0, \text{ for } D_S < x - \frac{D + L}{2}, \tag{8}$$

$$\frac{\sigma(x, 1)}{D^2} = \frac{\pi}{4}\left[1 - \lambda + 2\left(\frac{x}{D}\right)\right]\left[1 + \lambda + 2q - 2\left(\frac{x}{D}\right)\right], \text{ for } x - \frac{D + L}{2} \leq D_S < 2x - L, \tag{9}$$

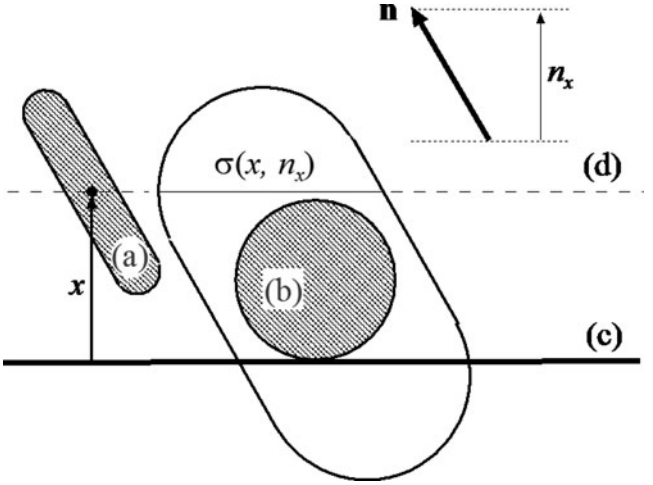

Figure 5. Schematic illustration of relation of (a) spherocylinder, (b) spheres and (c) the substrate. Dashed line indicates a plane (d) on which the center of the spherocylinder of distance x from the substrate moves. The sphere and the spherocylinder are hatched. Further explanation is noted in the text.

where $\lambda = L/D$ and $q = D_S/D$,

$$\frac{\sigma(x,1)}{D^2} = \frac{\pi}{4}(1+q)^2, \text{ for } 2x - L \le D_S < 2x + L, \tag{10}$$

$$\frac{\sigma(x,1)}{D^2} = \frac{\pi}{4}\left[1 + 2q - \lambda - 2\left(\frac{x}{D}\right)\right]\left[1 + \lambda + 2\left(\frac{x}{D}\right)\right], \text{ for } 2x + L \le D_S, \tag{11}$$

$$\sigma(x,0) = 0, \text{ for } D_S < x - \frac{D}{2}, \tag{12}$$

$$\frac{\sigma(x,0)}{D^2} = \pi R^2 + 2\lambda R, \text{ for} x - \frac{D}{2} \le D_S, \tag{13}$$

where

$$R^2 = \frac{1}{4}\left[1 + 2\left(\frac{x}{D}\right)\right]\left[1 + 2q - 2\left(\frac{x}{D}\right)\right]. \tag{14}$$

In a dilute limit, entropy s for a spherocylinder on the plane (d) of Fig. 5 is estimated as

$$s(x, n_x) = \frac{k_B}{\nu}\ln\frac{(\Omega\delta - \nu_S\sigma\delta)^\nu}{\nu!} \cong -k_B\left[\phi_S\sigma(x, n_x) + ln\rho - 1\right], \tag{15}$$

where Ω is area of the substrate (and also area of the plane (d) of Fig. 5), ν_S number of spheres on the substrate, ν number of spherocylinders on the plane (d) of Fig. 5, δ the thickness of the plane (d), ϕ_S number density per area of spheres, and ρ number density of spherocylinders per volume.

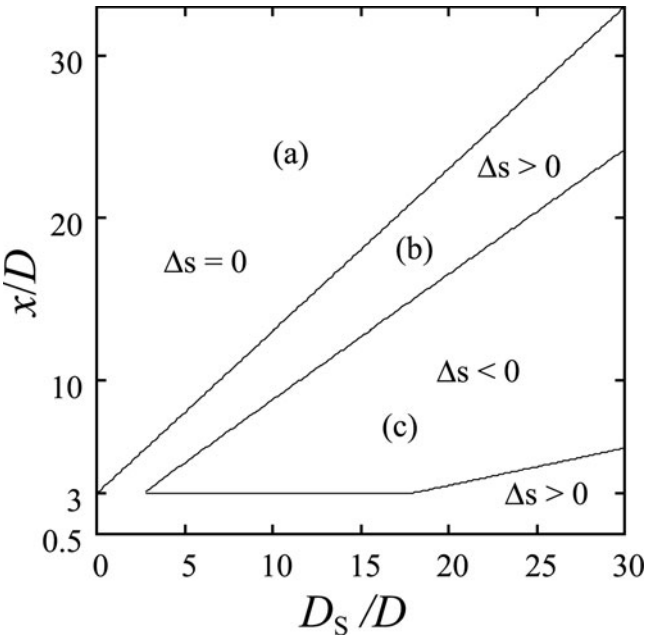

Figure 6. The sign of Δs depending on x and D_S for $L/D = 5$.

Entropy difference Δs from homeotropic structure to homogeneous structure is given by

$$\frac{\Delta s}{k_B \phi_S} = \frac{s(x,0) - s(x,1)}{k_B \phi_S} = \sigma(x,1) - \sigma(x,0). \tag{16}$$

Using Eqs. (8)–(14) and (16) we numerically examined the sign of Δs depending on x and D_S for $L/D = 5$. Figure 6 shows a diagram of the sign of Δs on the D_S vs. x plane.

The region (a) of Fig. 6 is determined by

$$x > D_S + \frac{D+L}{2}.$$

Spheres on the substrate do not affect spherocylinders in the region (a) for which the entropy increase Δs caused by the change from homeotropic alignment to homogeneous alignment is zero. Spherocylinders in the region (b) in which $\Delta s > 0$ contribute for stability of homogeneous alignment and those in the region (c) in which $\Delta s < 0$ contribute for stability of homeotropic alignment. Comparative increase of stability of homeotropic structure $n_x = 1$ of Fig. 4 for D_S between $4D$ and $8D$ is explained by the appearance of the region (c) of Fig. 6 at about $D_S = 4$. We expect that enhancement of region (b) due to increasing D_S causes the decrease of n_x at $D_S = 9$ of Fig. 4.

4. Conclusion

We examined how the surface conditions affected liquid crystal alignment by using Monte Carlo simulation. The flat surface was modified by adsorbed spheres and liquid crystal was modeled by hard spherocylinders. Figure 3 indicated that a final structure depended

on an initial configuration even for the same system parameters. In Fig. 4, we examined stability of homeotropic structure through change in director after an elapsed MC steps. We explained results considering excluded volume effect in Fig. 6.

In order to discuss detail of the stability, we have to calculate the free energy of each structure. However, for the stage of the present study, we did not calculate the free energy. As indicated by FIG. 3(a), we observed the cases in which an initial homeotropic structure was canceled after relaxation. However we have not observed any case in which an initial homogeneous structure is canceled in the nematic phase. So we expect that homogeneous alignment is comparatively favored than homeotopic alignment for the present systems of spheres on the plate and liquid crystalline spherocylinders.

References

[1] Park, B., Jung, Y., Choi, H.-H., Hwang, H.-K., Kim, Y., Lee, S., Jang, S.-H., Kakimoto, M., & Takezoe, H. (1998), *Jpn. J. Appl. Phys.*, *37*, 5663.
[2] Usami, K., Sakamoto, K., & Ushioda, S. (2004), *Mol. Cryst. Liq. Cryst.*, *412*, 219.
[3] Chaudhari, P., *et al.* (2001), *Nature*, *411*, 56.
[4] Momoi, Y., Kwak, M., Choi, D., Choi, Y., Jeong, K., Koda, T., Haba, O., Yonetake, K. (2012), *J. Soc. Inf. Display*, *20*, 486.
[5] Haba, O., Hiratsuka, D., Shiraiwa, T., Koda, T., Yonetake, K., Momoi, Y., & Furuta, K. (2013), *Mol.Cryst. Liq. Cryst.*, *574*, 84.
[6] Haba, O., Hiratsuka, D., Shiraiwa, T., Funakoshi, N., Awano, H., Koda, T., Takahashi, T., Yonetake, K., Kwak, M., Momoi, Y., Kim, N., Hong, S., Kang, D., & Choi, Y. (2014), *Opt. Mater. Express*, *4*, 934.
[7] Jeng, S.-C., Kuo, C.-W., Wang, H.-L. & Liao, C.-C. (2007), *Appl. Phys. Lett.*, *91*, 061112.
[8] Kuo, C.-W., Jeng, S.-C., Wang, H.-L., & Liao, C.-C. (2007), *Appl. Phys. Lett.*, *91*, 141103.
[9] Kim, D.Y., Kim, S., Lee, S.-A, Choi, Y.-E., Yoon, W.-J., Kuo S.-W., Hsu, C.-H., Huang, M., Lee, S. H., & Jeong K.-U. (2014), *J. Phys. Chem. C*, *118*, 6300.
[10] McGrother, S. C., Williamson, D. C., & Jackson, G. (1996), *J. Chem. Phys.*, *104*, 6755.
[11] Bolhuis, P., Frenkel, D., (1997), *J. Chem. Phys.*, *106*, 666.
[12] Stroobants, A., Lekkerkerker, H. N. W., & Frenkel, D. (1987), *Phys. Rev. A*, *36*, 2929.